*Journal of Statistical Physics, Vol. 42, Nos. 3/4, 1986*

# A New Integral Equation for the Radial Distribution Function of a Hard Sphere Fluid

**M. F. Wehner[1,2] and W. G. Wolfer[1]**

*Received October 9, 1984; revision received April 1, 1985*

Based on a proposal by Shinomoto, a new integral equation is derived for the radial distribution function of a hard-sphere fluid using mainly geometric arguments. This integral equation is solved by a perturbation expansion in the density of the fluid, and the results obtained are compared with those from molecular dynamics simulations and from the Born–Green–Yvon (BGY) and Percus–Yevick (PY) theories. The present theory provides results for the radial distribution function which are intermediate in accuracy between those obtained from the BGY and from the PY theories.

**KEY WORDS:** Hard sphere fluid; radial pair distribution function; perturbation solution.

## 1. INTRODUCTION

The radial pair distribution function is of fundamental importance in describing a dense fluid system in thermodynamic equilibrium. Formally, the pair distribution function is intimately connected to a hierarchy of many-body distribution functions. Presently, there exist several possible alternatives to break this hierarchy and arrive at an approximate solution. It is the purpose of this paper to explore a new way to determine the pair distribution function of a dense fluid and to compare it with previous approaches.

Among these previous approaches, the Born–Green–Yvon (BGY) hierarchy of equations relates the $s$-particle distribution function to the $(s+1)$-particle distribution function for a general choice of $s$. Choosing

[1] Fusion Technology Institute, 1500 Johnson Drive, University of Wisconsin–Madison, Madison, Wisconsin 53706.

[2] Current address: Lawrence Livermore National Laboratory, Livermore, California 94550.



0022-4715/86/0200-0493$05.00/0 

$s=2$ and utilizing a superposition approximation to express the three-particle distribution function in terms of the pair distribution function then yields the BGY equation for the radial pair distribution function, $g(r)$,

$$-k_B T \nabla_1 \ln\{g(r_{12})\} = \nabla_1 V(r_{12}) + n \int dq_3\, g(r_{13})\, g(r_{23})\, \nabla_1 V(r_{13}) \qquad \text{(BGY)}$$

where $V(r)$ is the interatomic potential and $r$ is the separation between particles.[2] This nonlinear integral equation has been extensively investigated via analytic and numerical procedures.[1,3,4]

Another approach, providing much better results, uses the connection between the thermodynamic partition function and the equilibrium distribution function to derive a completely different nonlinear integral equation. The Ornstein–Zernike equation relates the pair correlation function $[v(r)=g(r)-1]$ and the direct correlation function, $c(r)$, as[5]

$$v(r) = c(r) + n \int c(r')\, v(|\mathbf{r}-\mathbf{r}'|)\, dr' \qquad \text{(OZ)}$$

Although this expression is exact, a second independent relationship between the unknown functions is required to provide closure of the integral equation. This is provided by the Percus–Yevick (PY) approximation,[6]

$$c(r) = g(r)(1 - e^{V(r)/kT}) \qquad \text{(PY)}$$

or the hypernetted chain (HNC) approximation[7]

$$c(r) = g(r) - 1 - \ln[g(r)] - V(r)/kT \qquad \text{(HNC)}$$

Each of these is obtained by summing over a certain class of diagrams of an appropriate graphical expression. In principle the HNC approximation is the better of the two approximations since more diagrams are retained. However, in actual practice, the PY approximation provides far superior numerical results.[1] In the presence of a hard wall, the generalized mean spherical approximation[8] presents a further refinement of the Ornstein–Zernike approach.

Numerical experiments, using either Monte Carlo or molecular dynamics methods, provide the most "exact" results for the dense fluid system. In these types of numerical simulation, a many-body system is analyzed by recording the movement of all of the particles. Extensive results have been tabulated using the molecular dynamics approach for both the hard sphere potential[9] and for the more realistic Lennard-Jones interatomic potential.[10] Such calculations provide a useful comparison for

the various integral equation methodologies. In this paper, and the following one, we will use the geometrical arguments first proposed by Shinomoto[11] to find an equation of state for hard spheres against a hard wall and extend it to develop a new and completely different integral equation for $g(r)$ to describe the dense fluid system. Shinomoto's initial result was extremely compact and remarkably accurate. For this reason it has received some attention as a useful tool.[12,13] In addition, Shinomoto's original method suggests a perturbation solution of the new integral equation in terms of the packing fraction.

In Section 2, Shinomoto's theory of a hard sphere system is outlined and the new integral equation derived. In Section 3, the perturbation solution is developed to second order in the packing fraction, $y$. In Section 4, the results for the second-order pair distribution function are given. In Section 5, the third-order perturbation solution is derived. In Section 6, results for the third-order pair distribution are given. Finally, in Section 7, comparisons between this new integral equation and the existing integral equation theories of liquids are discussed.

## 2. SHINOMOTO'S THEORY FOR A HARD-SPHERE GAS

Consider a gas of average atom density $n$ consisting of hard-sphere particles of radius $a$. Let $g(r)$ denote the radial distribution function defined in the usual manner such that $4\pi n g(r) r^2\, dr$ is the number of particles to be found between the radii $r$ and $r+dr$ from the center of any test particle. Instead of the radial distance $r$ we may also use the distance $x = r - a$ from the surface of the test particle to the centers of surrounding atoms, and we may write instead

$$g(r) = g_a(x) \tag{1}$$

If the test particle now has a different radius, say $R$, than all the other particles in the gas, we denote this radial distribution function by $g_R(x)$.

We now make the usual assumption that the radial distribution function can be represented in the form

$$g_R(x) = \exp[-\phi(x)/kT] \tag{2}$$

where $\phi(x)$ is given by

$$\phi(x) = -\int_{\infty}^{x} F(x')\, dx' \tag{3}$$

Here, $F(x)$ is the mean force exerted on a generic particle (indicated by the solid small circle in Figs. 1 and 2) located at a distance $x$ from the test par-

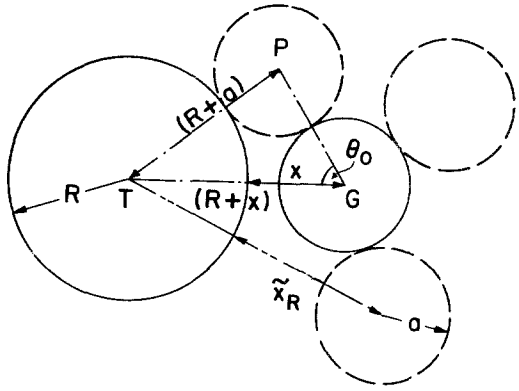


Fig. 1. Configuration of a convex "text particle" of radius $R$ surrounded by generic particles of radius $a$.

ticle's surface and $\phi(x)$ is the corresponding potential function. This force is the net action of the collisions of this generic particle at distance $x$ with all remaining particles surrounding it. These remaining particles are indicated by dashed circles when the "test particle" has a convex and a concave surface, respectively. The test particle's surface will represent the curved surface of the cavity or wall in later investigations.

The probability of finding one of the remaining particles in contact with the generic particle is assumed to be equal to the product of the probability of finding a particle at a distance $\tilde{x}_R$ from the surface of the test particle and the probability of two particles being in contact with one another. Hence, the density of these particles is $ng_a(a)\, g_R(\tilde{x}_R)$. This is, in

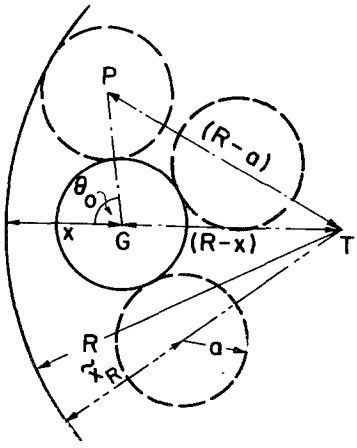


Fig. 2. Same as Fig. 1 except for a concave "test particle."

effect, the superposition approximation for the three-body distribution function. The remaining particles then exert on the generic particle the following net force in the direction perpendicular to the test particle's surface:

$$F(x) = 2\pi(2a)^2 nkTg_a(a) \int_{\theta_0(x)}^{\pi} g_R[\tilde{x}(x, \cos\theta)] \cos\theta \sin\theta \, d\theta \tag{4}$$

If the generic particle is at a distance $x < 3a$ from the test particle's surface, the impingement angle $\theta$ is limited to the range $\theta_0 \leqslant \theta \leqslant \pi$, where $\theta_0$ can be obtained from the triangle (TGP) in Figs. 1 and 2 by simple trigonometric considerations. The result is

$$\cos\theta_0(x) = \begin{cases} [(x \pm R)^2 + 4a^2 - (a \pm R)^2]/[4a(x \pm R)] & \text{for } a \leqslant x \leqslant 3a \\ 1 & \text{for } x \geqslant 3a \end{cases} \tag{5}$$

A similar trigonometric analysis gives the distance $\tilde{x}_R$ of one of the remaining particles from the test surface:

$$\tilde{x}_R(x, \cos\theta) = [(x \pm R)^2 + 4a^2 - 4a(x \pm R)\cos\theta]^{1/2} \mp R \tag{6}$$

The upper (lower) signs in Eqs. (5) and (6) apply to the convex (concave) test surface.

We may abbreviate the formulas somewhat by introducing the hard-sphere packing fraction

$$y = \frac{4\pi}{3} a^3 n \tag{7}$$

and the new integration variable

$$u = \cos\theta \tag{8}$$

Inserting Eq. (4) into Eq. (3) and subsequently into Eq. (2) we obtain an integral equation for the radial distribution function of the form

$$\ln g_R(x) = yg_a(a) \frac{6}{a} \int_{\infty}^{x} dx' \int_{-1}^{\cos\theta_0(x')} g_R[\tilde{x}_R(x', u)] u \, du \tag{9}$$

If we set $R = +a$, we obtain also an integral equation for the pair distribution function $g_a(x)$ given by

$$\ln g_a(x) = yg_a(a) \frac{6}{a} \int_{\infty}^{x} dx' \int_{-1}^{u_a(x')} g_a[\tilde{x}_a(x', u)] u \, du \tag{10}$$

where

$$u_a(x) = \begin{cases} (x+a)/4a & \text{for } a \leqslant x \leqslant 3a \\ 1 & \text{for } x \geqslant 3a \end{cases} \tag{11}$$

and

$$\tilde{x}_a(x, u) = [(x+a)^2 + 4a^2 - 4au(x+a)]^{1/2} - a \tag{12}$$

Equations (9) and (10) must be solved either numerically or by iteration. The latter method was chosen for the present paper, and it is described in the following section. Once $g_R(x)$ has been determined, the gas-kinetic pressure exerted on the curved test surface is given by

$$p = nkTg_R(a) \tag{13}$$

For a flat test surface, $R \to \infty$, Eq. (13) should reproduce the known results for the equation of state for a hard-sphere gas as obtained from either the existing integral equation theories or from molecular dynamics computer simulations. As Shinomoto has shown,[11] this is indeed the case. Although his equation of state is of different mathematical form, it gives practically identical results to the equation of state of Carnahan and Starling[14] for hard-sphere packing fractions $y \lesssim 0.47$.

## 3. PERTURBATION METHOD

Following the iteration procedure proposed by Shinomoto, we first assume pair and radial distribution functions valid to zero order in $y$ to be used in the right-hand side of Eq. (10). In doing so, we may then calculate the distribution functions valid to first order in $y$. Iterating on this procedure, the higher-order approximations may be found.

As the zero-order approximation, we assume that $g_a^0(1) \cong 1$ and $g_R^0(\tilde{x}) \cong 1$. This is a reasonable assumption for a dilute gas. Equation (4) then gives

$$F_1(x) = \begin{cases} -\dfrac{3}{a} ykT[1 - \cos^2\theta_0(x)] & \text{for } a \leqslant x \leqslant 3a \\ 0 & \text{for } x > 3a \end{cases} \tag{14}$$

which results in the effective pair potential

$$\phi_1(x) = \int_\infty^x F_1(x')\, dx' = \begin{cases} -ykT\psi_1(x) & \text{for } a \leqslant x \leqslant 3a \\ 0 & \text{for } x > 3a \end{cases} \tag{15}$$

where

$$\frac{1}{3}\psi_1(x)=\frac{1}{a}\int_x^{3a}[1-\cos^2\theta_0(x')]\,dx'=(3-\xi)-\frac{1}{16}\left\{\frac{1}{3}[(3+\rho)^3-(\xi+\rho)^3]\right.$$

$$\left.-2[(1+\rho)^2-4](3-\xi)-[(1+\rho)^2-4]^2[(3+\rho)^{-1}-(\xi+\rho)^{-1}]\right\} \quad (16)$$

and

$$\xi=x/a, \qquad \rho=\pm R/a \quad (17)$$

The radial distribution function in the first-order approximation is then given by

$$g_R^1(x)=\begin{cases}0 & \text{for } x<a\\ \exp[y\psi_1(x)] & \text{for } a\leqslant x\leqslant 3a\\ 1 & \text{for } x>3a\end{cases} \quad (18)$$

The pair distribution function $g_a(x)$ at contact, i.e., for $x=a$, is obtained from Eq. (18) by setting $R=+a$ or $\rho=+1$; accordingly

$$g_a^1(a)=\exp\left(\frac{5}{2}y\right) \quad (19)$$

In the next, i.e., second-order approximation, we use now Eqs. (12), (18) and (19) in Eq. (4) and compute an improved force function

$$F_2(x)=\frac{3y}{2a}kT\exp\left(\frac{5}{2}y\right)\int_{\theta_0}^{\pi}g_R^1[\tilde{x}(x,\cos\theta)]\cos\theta\sin\theta\,d\theta$$

$$=\frac{6}{a}ykT\exp\left(\frac{5}{2}y\right)\int_{\tilde{x}_0}^{\tilde{x}_1}g_R^1(\tilde{x})\,f(x,\tilde{x})\,d\tilde{x} \quad (20)$$

where

$$f(x,\tilde{x})=\frac{(x\pm R)^2-(\tilde{x}\pm R)^2+4a^2}{8a^2(x\pm R)^2}(\tilde{x}\pm R) \quad (21)$$

and

$$\tilde{x}_0=x-2a, \qquad \tilde{x}_1=x+2a \qquad \text{for } 3a<x<5a \quad (22)$$

and

$$\tilde{x}_0=a, \qquad \tilde{x}_1=x+2a \qquad \text{for } a\leqslant x\leqslant 3a$$

In order to evaluate the integral in Eq. (20) we make the low-density expansion

$$g_R^1(x) = \exp[y\psi_1(x)] \cong 1 + y\psi_1(x) \qquad \text{for } a \leqslant x \leqslant 3a \tag{23}$$

consistent with the first-order approximation. Then the second-order force function takes the form in Region I, $a < x < 3a$,

$$F_2(x) = N_2 \left[ \int_a^{x+2a} f(x, \tilde{x})\, d\tilde{x} + y \int_a^{3a} \psi_1(\tilde{x})\, f(x, \tilde{x})\, d\tilde{x} \right] \tag{24}$$

and in Region II, $3a < x < 5a$,

$$F_2(x) = N_2 \left[ \int_{x-2a}^{x+2a} f(x, \tilde{x})\, d\tilde{x} + y \int_{x-2a}^{3a} \psi_1(\tilde{x})\, f(x, \tilde{x})\, d\tilde{x} \right] \tag{25}$$

where $N_2 = (6ykT/a)e^{5/2y}$. The first term in Eq. (25) must vanish due to symmetry considerations. For $x > 5a$, $F_2(x) = 0$.

The effective potential in second order requires the additional integration

$$\phi_2(x) = \int_x^{5a} F_2(x')\, dx' \tag{26}$$

or in Region I, the solution of

$$\frac{\phi_2^{\mathrm{I}}(x)}{N_2} = \int_x^{3a} dx' \int_a^{x'+2a} d\tilde{x}\, f(x', \tilde{x}) + y \int_x^{3a} dx' \int_a^{3a} d\tilde{x}\, \psi_1(\tilde{x})\, f(x', \tilde{x}) + y \int_{3a}^{5a} dx' \int_{x'-2a}^{3a} d\tilde{x}\, \psi_1(\tilde{x})\, f(x', \tilde{x}) \tag{27}$$

and in Region II, the solution of

$$\frac{\phi_2^{\mathrm{II}}(x)}{N_2} = y \int_x^{5a} dx' \int_{x'-2a}^{3a} d\tilde{x}\, \psi_1(\tilde{x})\, f(x', \tilde{x}) \tag{28}$$

One must note that in order to be consistent in the second-order perturbation, the function, $e^{5y/2}$, must also be expanded in terms of $y$ and all terms in the final result involving powers greater than $y^2$ must be omitted. The radial distribution function in the second-order approximation is then given by

$$g_R^2(x) = \begin{cases} 0, & x \leqslant a \\ \exp[y\psi_2^{\mathrm{Ia}}(x) + y^2\psi_2^{\mathrm{Ib}}(x)], & a < x < 3a \\ \exp[y^2\psi_2^{\mathrm{II}}(x)], & 3a < x < 5a \\ 1, & x > 5a \end{cases} \tag{29}$$

where the functions in the arguments of the exponentials are defined by the integrals in Eqs. (27) and (28). Although the integrands of Eqs. (27) and (28) are elementary rational functions, the integrations become quite tedious for a general choice of $R$. For this reason, the symbolic manipulation program, REDUCE2, was used to perform the integrals.

## 4. SECOND-ORDER PAIR DISTRIBUTION FUNCTION

The second-order potential evaluated at $R = +a$ is given as

$$\frac{\phi_2^{\mathrm{I}}(x, y, R=a)}{ykT} = \left(1+\frac{5}{2}y\right)\left[-\frac{(x-3a)^2(x+9a)}{16a^3}\right] + y\left[\frac{3(69a^2+208ax-77x^2)}{70a(a+x)}+\frac{52}{35}\right] \tag{30}$$

for $a \leqslant x \leqslant 3a$ and by

$$\frac{\phi_2^{\mathrm{II}}(x, y, R=a)}{y^2kT} = \frac{(x-5a)^4(x^3+27ax^2+159a^2x+85a^3)}{2240a^6(x+a)} \tag{31}$$

for $3a \leqslant x \leqslant 5a$.

In Fig. 3, the second-order pair distribution function is plotted as a function of the reduced radius from the center of the test particle, $r/d$, for various packing fractions. Here, $d$ is the diameter of the particles and $r = x + a$. In Fig. 4, graphs of the pair distribution function based on the data from the molecular dynamics calculations of Alder and Hecht[9b] are shown for purposes of comparison. Agreement is quite good between the results shown in these two figures at densities low enough such that the characteristic second peak around $r/d = 2$ is not significant. In fact, the second-order approximation cannot reproduce such a peak as is evident at higher densities. This is a systematic result of the iteration procedure. The zeroth-order approximation assumed a uniform density of particles around the test particle. Geometrical considerations alone produce then an attractive averaged first-order force in the region $a < x < 3a$ of Fig. 1. Hence the pair distribution is enhanced in this region. In the second-order perturbation, the geometrical effects still produce attractive forces very near the test particle, but the enhanced first-order pair distribution causes averaged second-order forces which act in the opposite direction in the region farther away from the test particle. Such an opposing set of forces causes the

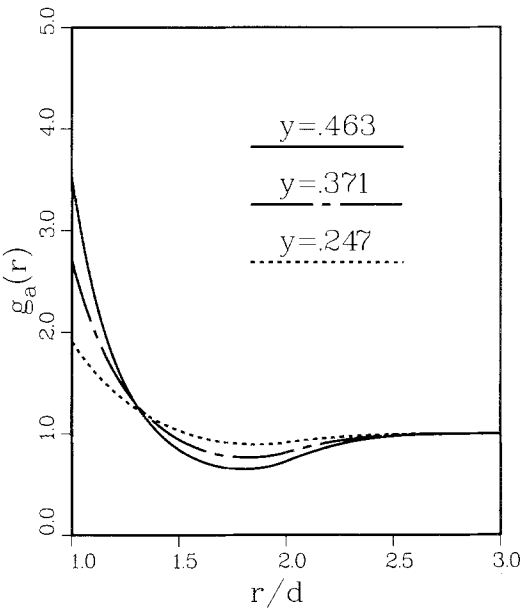


Fig. 3. The second-order perturbation solution of Eq. (10) evaluated at various packing fractions.

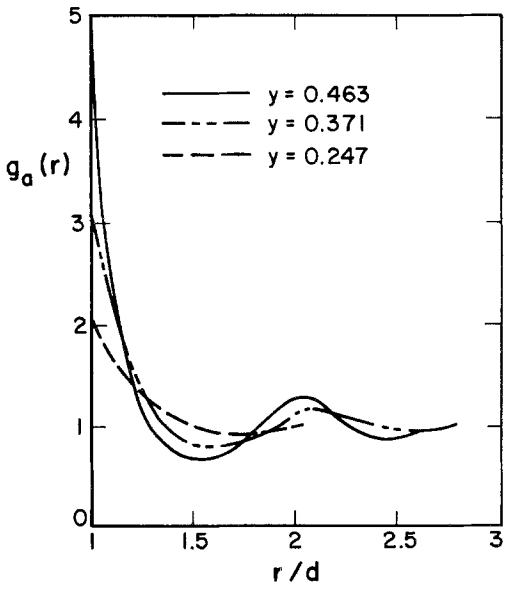


Fig. 4. The molecular dynamics calculations of Alder and Hecht for the pair distribution function at various packing fractions.

observed trough in the second-order pair distribution function. The second peak in the pair distribution function would be produced by the next(third)-order approximation as the localized depression in the density of particles would again reverse the direction of the averaged force around $x = 3a$ causing an enhancement in that region.

## 5. GENERAL THIRD-ORDER PERTURBATION SOLUTION

To carry out the third-order perturbation, we simply repeat the iteration procedure using the second-order radial distribution functions.

From Eq. (4), the third order averaged force is

$$F_3(x) = \frac{6ykT}{a} g_a^2(a) \int_{\tilde{x}_0}^{\tilde{x}_1} g_R^2(\tilde{x}) f(x, \tilde{x})\, d\tilde{x} \tag{32}$$

where the limits are defined in the same manner as before. Expanding Eq. (29) in powers of $y$ yields

$$g_R^2(x) = \begin{cases} 0, & x \leqslant a \\ 1 + y\psi_2^{\mathrm{Ia}}(x) + y^2\{\psi_2^{\mathrm{Ib}}(x) + \frac{1}{2}[\psi_2^{\mathrm{Ia}}(x)]^2\}, & a \leqslant x \leqslant 3a \\ 1 + y^2\psi_2^{\mathrm{II}}(x), & 3a \leqslant x \leqslant 5a \\ 1, & x \geqslant 5a \end{cases} \tag{33}$$

Inserting this expansion into Eq. (32) and integrating from $x$ to $7a$ yields the third-order potential. In a final step, $g_a^2(a)$ is also expanded about $y$. After the multiplications, terms of order greater than $y^3$ are dropped. Implementing these steps, one finds that in Region III, $5a \leqslant x \leqslant 7a$,

$$\frac{\phi_3^{\mathrm{III}}(x)}{N_3} = y^2 \int_x^{7a} dx' \int_{x'-2a}^{5a} d\tilde{x}\, f(x', \tilde{x})\, \psi_2^{\mathrm{II}}(\tilde{x}) \tag{34}$$

in Region II, $3a \leqslant x \leqslant 5a$,

$$\begin{aligned} \frac{\phi_3^{\mathrm{II}}(x)}{N_3} = \frac{\phi_3^{\mathrm{III}}(x = 5a)}{N_3} &+ y \int_x^{5a} dx' \int_{x'-2a}^{3a} d\tilde{x}\, \psi_2^{\mathrm{Ia}}(\tilde{x})\, f(x', \tilde{x}) \\ &+ y^2 \int_x^{5a} dx' \int_{x'-2a}^{3a} d\tilde{x}\, f(x', \tilde{x}) \left\{ \psi_2^{\mathrm{Ib}}(\tilde{x}) + \frac{1}{2}[\psi_2^{\mathrm{Ia}}(\tilde{x})]^2 \right\} \\ &+ y^2 \int_x^{5a} dx' \int_{3a}^{5a} d\tilde{x} f(x', \tilde{x})\, \psi_2^{\mathrm{II}}(\tilde{x}) \end{aligned} \tag{35}$$

and in Region I, $a < x < 3a$,

$$\frac{\phi_3^{\mathrm{I}}(x)}{N_3} = \frac{\phi_3^{\mathrm{II}}(x=3a)}{N_3} + \int_x^{3a} dx' \int_a^{x'+2a} d\tilde{x}\, f(x', \tilde{x}) + y \int_x^{3a} dx' \int_a^{3a} d\tilde{x} f(x', \tilde{x})\, \psi_2^{\mathrm{Ia}}(\tilde{x}) + y^2 \int_x^{3a} dx' \int_a^{3a} d\tilde{x} f(x', \tilde{x}) \times \left\{ \psi_2^{\mathrm{Ib}}(\tilde{x}) + \frac{1}{2} [\psi_2^{\mathrm{Ia}}(\tilde{x})]^2 \right\} + y^2 \int_x^{3a} dx' \int_{3a}^{x'+2a} d\tilde{x} f(x', \tilde{x})\, \psi_2^{\mathrm{II}}(\tilde{x}) \tag{36}$$

where

$$N_3 = \frac{6ykT}{a} g_a^2(a) \cong \frac{6ykT}{a} \left( 1 + \frac{5}{2} y + \frac{1009}{280} y^2 \right) \tag{37}$$

The radial distribution function in the third order is then

$$g_R^3(x) = \begin{cases} 0, & x < a \\ \exp\{ y\psi_3^{\mathrm{Ia}}(x) + y^2\psi_3^{\mathrm{Ib}}(x) + y^3\psi_3^{\mathrm{Ic}}(x) \}, & a < x < 3a \\ \exp\{ y^2\psi_3^{\mathrm{IIa}}(x) + y^3\psi_3^{\mathrm{IIb}}(x) \}, & 3a < x < 5a \\ \exp\{ y^3\psi_3^{\mathrm{III}}(x) \}, & 5a < x < 7a \\ 1, & x > 7a \end{cases} \tag{38}$$

It should be noted that in a consistent perturbation expansion the lower-order terms should remain unchanged with each perturbation. This is indeed the case as the relations

$$\begin{aligned} \psi_3^{\mathrm{Ia}}(x) &= \psi_2^{\mathrm{Ia}}(x) = \psi_1(x) \\ \psi_2^{\mathrm{Ib}}(x) &= \psi_3^{\mathrm{Ib}}(x) \end{aligned} \tag{39}$$

and

$$\psi_3^{\mathrm{IIa}}(x) = \psi_2^{\mathrm{II}}(x)$$

are found to hold.

## 6. THIRD-ORDER PAIR DISTRIBUTION FUNCTION

The integrals of Eqs. (34) to (36) have been performed numerically for the value $R = a$ to provide the third-order pair distribution function. The results are shown graphically in Fig. 5. Note that these curves exhibit the

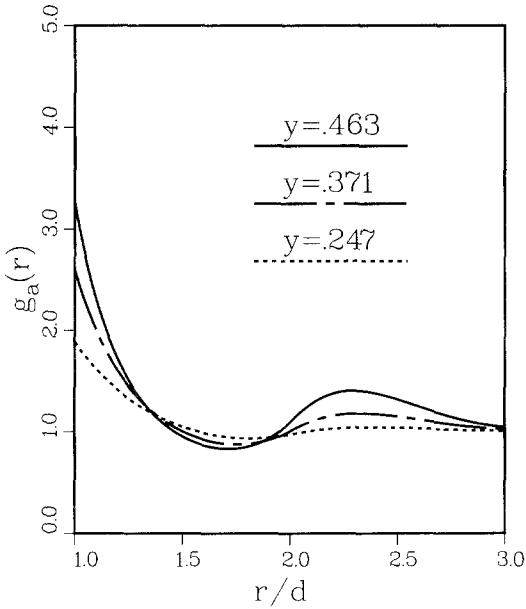


Fig. 5. The third-order perturbation solution of Eq. (10) evaluated at various packing fractions.

oscillatory behavior described in Section 4. Quantitatively, the comparison is better at the lower two densities. At $y = 0.463$, the contact value, i.e., $g(a)$, is noticeably too low and the location of the peaks and valleys too far to the right. This latter observation can be partially explained by the relatively low order of the perturbation solution. Note in Fig. 4, that the trend of the exact solution's first valley is to move to the left with increasing packing fraction. In Fig. 3, the second-order approximation, the minima are located roughly at the same value of $y$. But in the third-order approximation, the location of the first minimum does indeed follow the trend of the exact results, at least in a qualitative sense at the higher densities.

## 7. CONCLUSION AND DISCUSSION

Using solely the geometrical arguments first proposed by Shinomoto,[11] we have derived a new integral equation for the radial distribution function of a hard-sphere dense fluid system. Extending Shinomoto's original method provides a perturbation solution to this nonlinear integral equation.

As far as the relationships between this new integral equation and the existing theories of dense fluids are concerned, the BGY approach is by far the most similar. As in the development leading to Eq. (9), the BGY equation can be derived by considering the forces acting on a test particle.[15] To illustrate the differences between the two formalisms more explicitly, consider the BGY equation for hard spheres under the superposition approximation as[3,16]

$$\ln g_a(x) = \frac{\pi n}{2a(x+a)} \int_{\max(a,x-2a)}^{x+2a} \left[ \frac{(x-s)^2}{4a^2} - 1 \right] (s+a)[g_a(s)-1]\, ds \tag{40}$$

We may rewrite the double integral equation (9) as a single integral equation by reversing the integration order. Then, Shinomoto's geometric model can be described by

$$\ln g_R(x) = -\frac{6y}{a} g_a(a) \int_{\max(a,x-2a)}^{x+2a} d\tilde{x}\, g_R(\tilde{x})\, k_R(x,\tilde{x}) \tag{41}$$

where

$$k_R(x,\tilde{x}) = \int_x^{\tilde{x}+2a} dx'\, f(x',\tilde{x})$$

In the limit that $R \to a$, the kernel becomes

$$k_a(x',\tilde{x}) = \frac{(\tilde{x}+a)}{8a^2} \left[ 2\tilde{x} + a - \frac{(\tilde{x}+a)^2 + (x+2a)(x-a) - 2a^2}{x+a} \right] \tag{42}$$

Although both theories are described by similar nonlinear integral equations of the second kind there are some fundamental differences. Most importantly the appearance of the pair correlation function instead of the pair distribution function in the BGY formalism causes Eq. (40) to be inhomogeneous. In contrast, there are no such terms in the current formalism, resulting in a homogeneous integral equation. In addition to this, the BGY kernel is of a polar type and can be made symmetric by the transformation $g_a(x) = h(x)/(x+a)^2$.[17] No apparent transformation exists for the kernel of Eq. (42).

In addition to these differences in form, the solutions also behave in different manners at extremely high (unphysical) densities. The numerical solutions of the hard-sphere BGY equation do not converge or yield physically acceptable solutions at such high densities. This fact, confirmed by molecular dynamics studies, suggests a phase transition near $y = 0.47$.[15] It is not fully understood what the cause of this behavior is. However, such behavior is not exhibited by the third-order perturbation solution of Eq. (9) or by the other integral equation approaches.

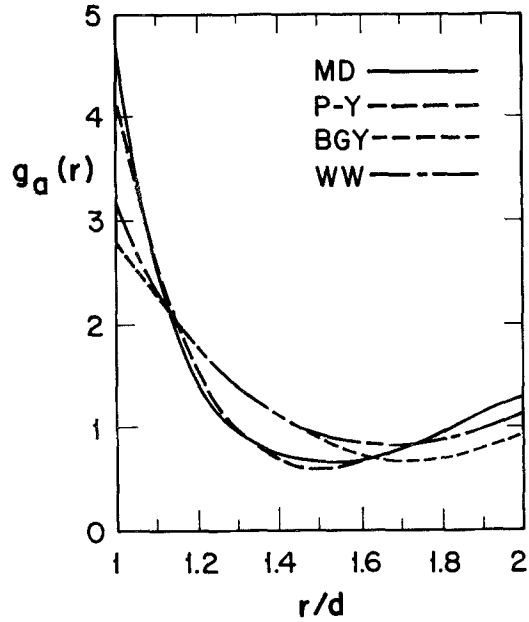


Fig. 6. A graphical comparison of some of the various hard-sphere pair distribution approaches at the packing fraction $y = 0.463$. MD is the molecular dynamics results of Alder and Hecht. PY is the Wertheim–Thiele solution of the Percus–Yevick equation. BGY is the numerical solution of the Born–Green–Yvon equation. WW is the third-order perturbation solution of Eq. (10).

A graphical comparison of the pair distribution functions produced by the various dense fluid theories is given in Fig. 6 together with the "exact" molecular dynamics results.[1] It should be noted that the third-order perturbation solution of Eq. (9) produces results slightly more accurate than the BGY approach but less accurate than the Wertheim–Thiele solution of the PY equation. At this high density ($y = 0.463$), terms of higher order than 3 probably contribute significantly to the solution of Eq. (9). Therefore, a numerical evaluation of Eq. (9) is required at high densities before a final comparison can be made. Nevertheless, the present results indicate that this new approach to the theory of fluids is a promising one.

## ACKNOWLEDGMENT

The authors would like to thank Professor J. K. Percus for his encouragement and useful comments regarding this approach.

This research was supported by the U.S. Department of Energy under contract No. DE-AC02-82ER52082 with the University of Wisconsin.

## REFERENCES


1. R. Balescu, *Equilibrium and Nonequilibrium Statistical Mechanics* (Wiley, New York, 1975).
2. M. Born and H. S. Green, *Proc. R. Soc.* **A188**:10 (1946).
3. J. G. Kirkwood, E. K. Maun, and B. J. Alder, *J. Chem. Phys.* **18**:1040 (1950).
4. B. Borstnik, D. Janezic, and A. Azman, *Mol. Phys.* **42**:721 (1981).
5. L. S. Ornstein and F. Zernike, *Proc. Acad. Sci. Amsterdam* **17**:793 (1914).
6. (a) J. K. Percus and G. J. Yevick, *Phys. Rev.* **110**:1 (1958); (b) E. Thiele, *J. Chem. Phys.* **39**:474 (1963); (c) M. S. Wertheim, *Phys. Rev. Lett.* **10**:321 (1963); *J. Math. Phys.* **5**:643 (1964). (d) W. Smith and D. Henderson, *Molec. Phys.* **19**:411 (1970).
7. T. Morita and K. Hiroike, *Prog. Theory. Phys.* **23**:1003 (1960).
8. E. Waisman, D. Henderson, and J. Lebowitz, *Molec. Phys.* **32**:1373 (1976).
9. (a) B. J. Alder and T. Wainwright, *J. Chem. Phys.* **27**:1209 (1957); (b) B. J. Alder and C. E. Hecht, *J. Chem. Phys.* **50**:2032 (1969).
10. (a) A. Rahman, *Phys. Rev.* **136**:A405 (1964); (b) L. Verlet, *Phys. Rev.* **159**:98 (1967); *Phys. Rev.* **165**:201 (1968).
11. S. Shinomoto, *Phys. Lett.* **89A**:19 (1982).
12. J. K. Percus, *J. Chem. Phys.* **79**:3009 (1983).
13. J. K. Percus, private communication.
14. N. F. Carnahan and K. E. Starling, *J. Chem. Phys.* **51**:635 (1969).
15. C. Croxton, *Liquid State Physics—A Statistical Mechanics Introduction* (Cambridge University Press, London, 1974).
16. J. MacCarthy, J. Kozak, K. Green, and K. Luks, *Mol. Phys.* **44**:17 (1981).
17. P. M. Morse and H. Feshbach, *Methods of Theoretical Physics, Vol. 1* (McGraw-Hill, New York, 1953).